2862–2868 *Nucleic Acids Research, 2012, Vol. 40, No. 7* *Published online 10 December 2011*
doi:10.1093/nar/gkr1173

Quantitative prediction of 3D solution shape and flexibility of nucleic acid nanostructures

Do-Nyun Kim[1], Fabian Kilchherr[2], Hendrik Dietz[2,*] and Mark Bathe[1,*]

[1]Laboratory for Computational Biology & Biophysics, Department of Biological Engineering, Massachusetts Institute of Technology, Cambridge, MA 02139, USA and [2]Department of Physics & Walter Schottky Institute, Center for Integrated Protein Science, Technische Universität München, Garching, Germany

Received September 13, 2011; Revised November 10, 2011; Accepted November 11, 2011

ABSTRACT

DNA nanotechnology enables the programmed synthesis of intricate nanometer-scale structures for diverse applications in materials and biological science. Precise control over the 3D solution shape and mechanical flexibility of target designs is important to achieve desired functionality. Because experimental validation of designed nanostructures is time-consuming and cost-intensive, predictive physical models of nanostructure shape and flexibility have the capacity to enhance dramatically the design process. Here, we significantly extend and experimentally validate a computational modeling framework for DNA origami previously presented as CanDo [Castro,C.E., Kilchherr,F., Kim,D.-N., Shiao,E.L., Wauer,T., Wortmann,P., Bathe,M., Dietz,H. (2011) A primer to scaffolded DNA origami. *Nat. Meth.*, 8, 221–229.]. 3D solution shape and flexibility are predicted from basepair connectivity maps now accounting for nicks in the DNA double helix, entropic elasticity of single-stranded DNA, and distant crossovers required to model wireframe structures, in addition to previous modeling (Castro,C.E., *et al.*) that accounted only for the canonical twist, bend and stretch stiffness of double-helical DNA domains. Systematic experimental validation of nanostructure flexibility mediated by internal crossover density probed using a 32-helix DNA bundle demonstrates for the first time that our model not only predicts the 3D solution shape of complex DNA nanostructures but also their mechanical flexibility. Thus, our model represents an important advance in the quantitative understanding of DNA-based nanostructure shape and flexibility, and we anticipate that this model will increase significantly the number and variety of synthetic nanostructures designed using nucleic acids.

INTRODUCTION

Programmable self-assembly of complementary single-stranded nucleic acids is a versatile approach to designing sophisticated nanoscale structures (2–4). Scaffolded DNA origami is a successful approach that enables construction of DNA-based nanostructures in which hundreds of 'staple' oligonucleotides hybridize with a 'scaffold' strand that is several-thousand-bases long. This structure then consists of numerous double-helical domains linked via covalent phosphate linkages into a complex 3D geometry (1,5–11).

Designing DNA nanostructures to meet structural and mechanical specifications is a formidable task even for experts in the field due largely to the lack of predictive computational design frameworks. For example, slight geometrical incompatibilities between parallel double-helical DNA domains superpose to induce global shape deformations including twist and bend (7). While such deformations are intuitive for simple shapes, they become highly non-intuitive when heterogeneous combinations of twist-stretch-bend are present. Further, nanostructures are subject to significant thermal forces in solution that disorder the structure. Accounting quantitatively for thermally induced shape fluctuations is important to applications requiring nanometer-scale control over target shape. Given the substantial time and financial cost associated with the manual design and experimental validation of designed nanostructures, predictive computational tools are of great use for increasing the number and variety of DNA-based nanostructures produced.

*To whom correspondence should be addressed. Tel: +1 617 324 5685; Fax: +1 617 324 7554; Email: mark.bathe@mit.edu
Correspondence may also be addressed to Hendrik Dietz. Tel: +49 89 289 11615; Fax: +49 89 289 11612; Email: dietz@tum.de

To meet this need, we previously developed a computational modeling framework to predict the 3D solution shape and flexibility of DNA-based nanostructures (1). While this model accounted for the canonical bend, twist, and stretch stiffness of the DNA double helix, it ignored important effects including backbone nicks in DNA strands, entropic elasticity of single-stranded DNA used to design, for example, tensegrity structures (11), and distant crossovers used in wireframe structures (7). Here, we significantly extend this modeling framework to include these features of DNA nanostructure designs, and systematically validate experimentally its prediction of nanostructure solution shape and flexibility.

METHODS

Negative-stain TEM image analysis

Samples were applied to glow-discharged (Glow discharger EMS 100, Electron Microscopy Sciences) carbon-coated TEM grids (EFCF400-Cu-50, Electron Microscopy Sciences) and negative-stained with a 2% uranyl formate stain solution including 0.5% 5 M sodium hydroxide solution. Transmission electron micrographs were taken with a Philips CM100 transmission electron microscope operated at 100 kV. Single particle libraries were generated from micrographs taken at a magnification of 28 500 by boxing individual particles

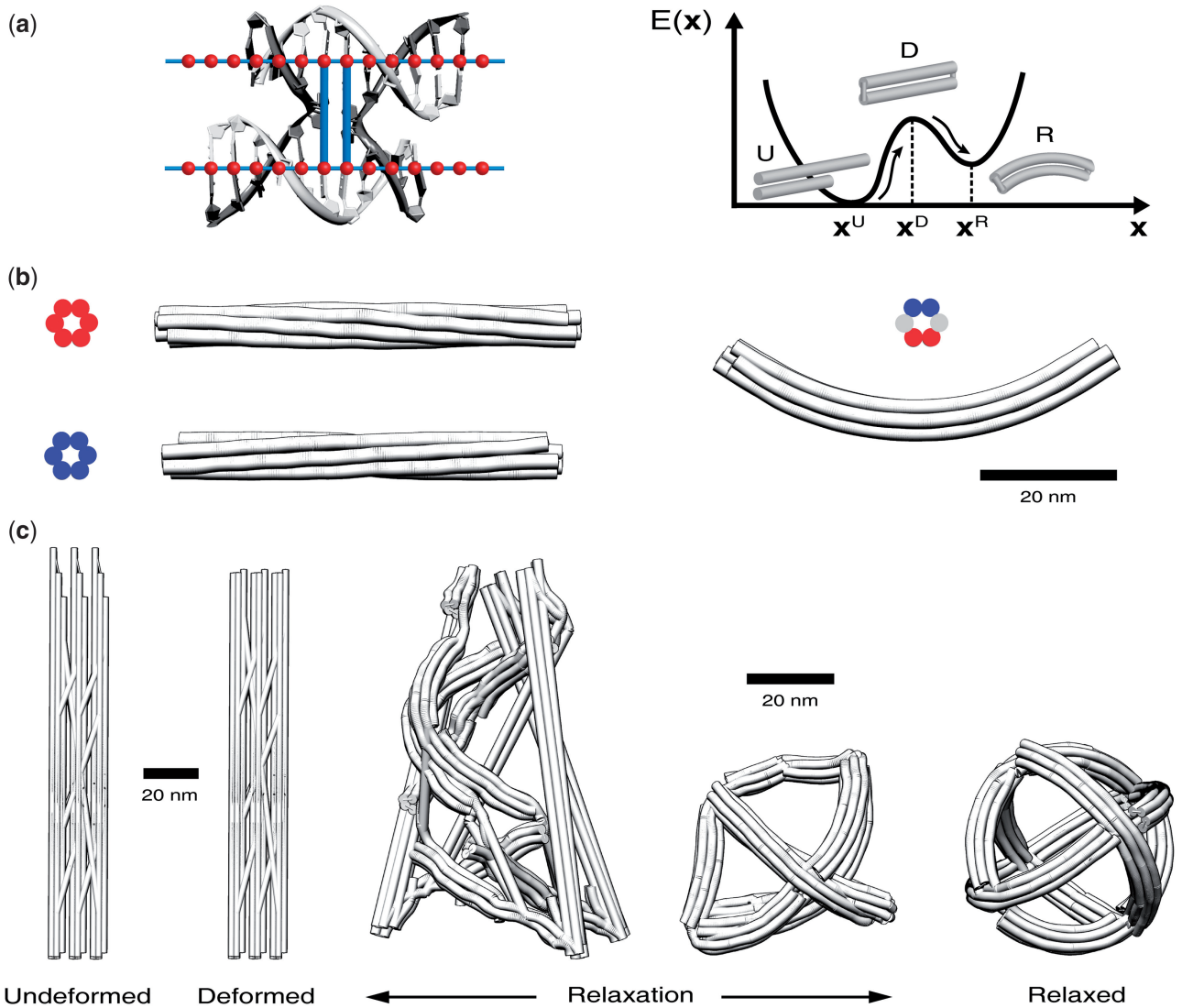

Figure 1. Prediction of 3D solution shape of non-linear DNA-based nanostructures. (**a**) DNA double helices are treated as isotropic elastic rods connected by rigid crossovers (left). Spheres correspond to finite element nodes used to describe the position and orientation of DNA basepairs, and lines represent finite element beams that model the stretching, twisting and bending mechanics of DNA. 3D solution shape is computed using a mechanical energy perturbation in which double helices are first deformed via stretching and twisting until crossover locations are in register, followed by energy minimization (right). The undeformed, deformed and mechanically relaxed (equilibrium) conformations of the DNA nanostructure are denoted U, D and R in the schematic at right. (**b**) Example deformations induced by mismatch between neighboring DNA helices induced by (red) insertions and (blue) deletions for a honeycomb lattice bundle (Supplementary Figures S2 and S17). (**c**) Snapshots of a spherical wireframe structure (7) during the deformation and relaxation process.

with the boxer routine of EMAN2 (12). Particles with obvious defects were omitted. Second, a reference particle was chosen out of the library and each individual particle of the library was aligned against the reference particle using the multi-ref-align routine of IMAGIC 4.0 (Imagic software, Image Science Software GmbH, Berlin, Germany). The new libraries with aligned particles were re-inspected and incorrectly aligned particles were removed. Finally, average and variance images were obtained with the *sum-images* routine of IMAGIC 4.0.

Computational model for nucleic acid shape and mechanics

DNA origami nanostructures are modeled as bundles of isotropic elastic rods that are rigidly constrained to their nearest neighbors at specific crossover positions. Each rod consists of a set of two-node beam finite elements representing the stretching (1 100 pN), bending (230 pN nm^2), and torsional (460 pN nm^2) stiffness of the B-form DNA double helix. Nicks are modeled by reducing backbone bending and torsional stiffness by a factor of 100 whereas stretching stiffness is retained at double-helix values. The value of 100 was chosen empirically based on a comparison of solution shapes with extensive nicks with experimental TEM images, and is also consistent with the base-stacking free energy of DNA (13). A more sophisticated model might employ distinct stiffnesses for the unruptured and ruptured states of the double-helix backbone instead of a single, reduced backbone stiffness, which may be the subject of future work. The position and orientation of DNA basepairs are represented by beam finite element nodal degrees of freedom. Connections between double helices formed from single-stranded DNA are treated as non-linear springs that model the force-extension behavior of the modified freely jointed chain model (14) (Supplementary Note 1). This approximation is valid for worm-like chains with a persistence length that is considerably smaller than the chain contour length. Distant crossovers used in wireframe structures are modeled as stiff beams that gradually shrink during the perturbation analysis until their length reduces to the distance between neighboring helices or the helix diameter. Relative orientations of helices connected by distant crossovers are unconstrained so that our model is limited at present to on-lattice modeling of DNA origami structures. The mechanical perturbation analysis used to compute the equilibrium solution shape begins with the undeformed conformation of the DNA origami structure designed on a honeycomb or square lattice. Helices are arranged in parallel on the lattice using standard B-form DNA geometric parameters (helix diameter of 2.25 nm, helicity of 10.5 basepairs per turn, and axial rise of 0.34 nm per basepair). The structure is initially deformed as shown in Figure 1 to eliminate axial and torsional mismatch between neighboring helices, and subsequently rigid constraints are applied to fully constrain all degrees of freedom of neighboring helices at crossover locations. The final solution shape is computed iteratively using the commercial finite element software program ADINA (Automatic Dynamic Incremental Non-linear Analysis, ADINA R&D Inc., Watertown, MA, USA) using a geometrically non-linear finite element formulation to reach mechanical equilibrium. Normal mode analysis (15,16) is performed at this mechanical free energy minimum to compute the mechanical flexibility of the folded structure. Root-mean-square fluctuations of basepairs are computed at 298 K for the final solution shape using 200 lowest normal modes and the equipartition theorem of statistical thermodynamics (17). The time required to compute these deformed shapes ranges from 5 to 35 min on an Intel® Core™ i7 processor with 12 GB RAM.

Double-helical DNA is treated as a homogeneous, isotropic elastic rod. Sequence-dependent mechanical properties (18), interhelical electrostatic repulsion, and the major–minor groove of DNA are ignored. Single-stranded DNA connecting double-helical domains is treated as an entropic spring (14) (Supplementary Note 1) and nicks in DNA strand backbones are modeled using reduced bending and torsional stiffness compared with non-nicked double-helical DNA (Figure S1). Phosphate backbone strand crossovers are modeled as rigid links of zero length (Figure 1a). To compute the 3D shape of the DNA nanostructure, the

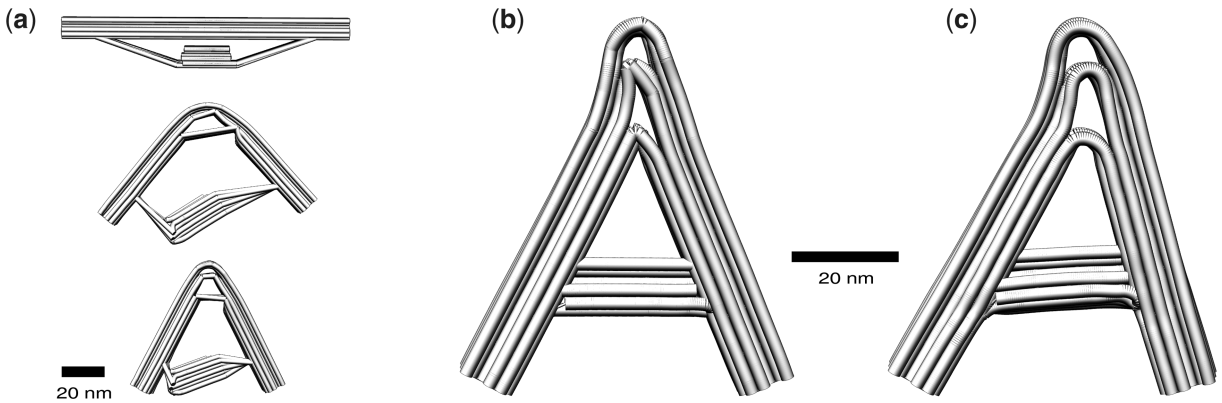

Figure 2. Effect of nicks on 3D solution shape. (**a**) Snapshots of 'A'-like object during the deformation and relaxation process. (**b** and **c**) Predicted solution shapes of an 'A'-like object (**b**) including the nick model and (**c**) ignoring the nick model.

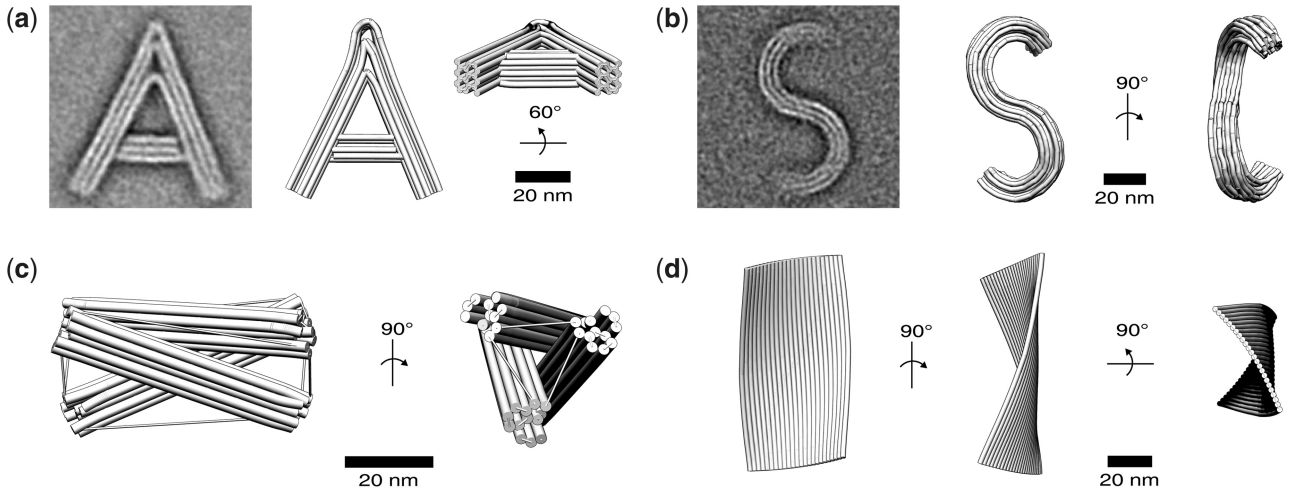

Figure 3. Experimental validation of non-linear solution shapes of DNA nanostructures. (**a** and **b**) TEM images (left) and predicted solution shapes (middle and right) for objects resembling capital letters 'A' and 'S' (Supplementary Figures S18–S19). TEM images are obtained by averaging single particle images (Supplementary Figures S4–S5). (**c**) Predicted solution shapes of a tensegrity structure (11). (**d**) Predicted solution shapes of a single-layer rectangular structure (5).

procedure performs a mechanical perturbation analysis in which DNA domains are simultaneously relaxed from their initial structure, assumed to reside on a honeycomb or square lattice, to their minimum mechanical free energy shape (Figure 1a). To achieve this, neighboring helices are first deformed in the axial and torsional directions to align strand crossovers assuming an average B-form DNA helicity of 10.5 bp per turn (19). Crossover constraints are then applied between neighboring helices and the structure is relaxed iteratively using a finite element approach that is well established in the structural mechanics field (20). The initial structure assumes internal registry of backbone positions compatible with the honeycomb-type or square-lattice packing (6,7).

RESULTS AND DISCUSSION

Application of the procedure to a simple 6-helix honeycomb unit cell of 178-basepair length illustrates its ability to predict intuitive shapes induced by site-directed mismatches in crossover positions (Figure 1b and Supplementary Figure S2). Application to a complex 3D wireframe structure that involves highly non-linear mechanical energy perturbations illustrates the model's predictive power when non-intuitive shape distortions are accompanied by significant local buckling and distortions along the computed mechanical perturbation pathway (Figure 1c and Supplementary Figure S3). Such calculations of the solution shapes of wire-frame structures including distant crossovers were impossible with our previous model (1).

To further explore its ability to predict wireframe topology shapes, we built a novel multi-layer DNA origami structure that resembles a capital letter 'A' (Figures 2, 3a and Supplementary Figure S4). This object has a complex wireframe topology with a final structure that is distant from the initial structure used for the perturbation analysis in our model. The model correctly predicts the global shape within obvious experimental error, despite the high non-linearity involved in the mechanical perturbation pathway (Figure 2a). This shape illustrates the importance of modeling nicks because the symmetric 'A' shape (Figures 2b and 3a) observed experimentally is not obtained when nicks are ignored (Figure 2c). We also designed and built a novel multi-layer DNA origami structure resembling the capital letter 'S' (Figure 3b and Supplementary Figure S5), which includes two domains of opposite curvature. Again, the model correctly predicts the global structure including a precise match of curvature within experimental error. Importantly, the model also predicts an out-of-bending-plane twist deformation that is unfortunately invisible in the experimental data because 'S' particles adhere to the TEM support surface in the flat orientation shown in Figure 3b. The object's curvature was designed by balanced insertions and deletions that cancel right-handed and left-handed torques induced by local over- and underwinding in the structure (7). However, this computational result suggests that these torques are in fact unbalanced because of distinct internal torques of double-helical DNA segments of different length that are over- or underwound by the same twist angle. This result illustrates a non-intuitive feature of 3D shape that is likely to be present in solution but may remain unnoticed experimentally due to limitations in imaging 3D shape.

DNA origami objects packed on the square lattice have been shown to exhibit global twist deformation in the absence of insertions and deletions due to underwinding of double helices with an average helicity of 10.67 bp per turn (21). This is in contrast to honeycomb lattice structures that appear undeformed when crossovers are spaced at intervals of 10.5 bp per turn (7). To test the ability of our model to predict the influence of lattice geometry on overall shape, we analyzed a set of multi-layer DNA origami blocks designed on a square

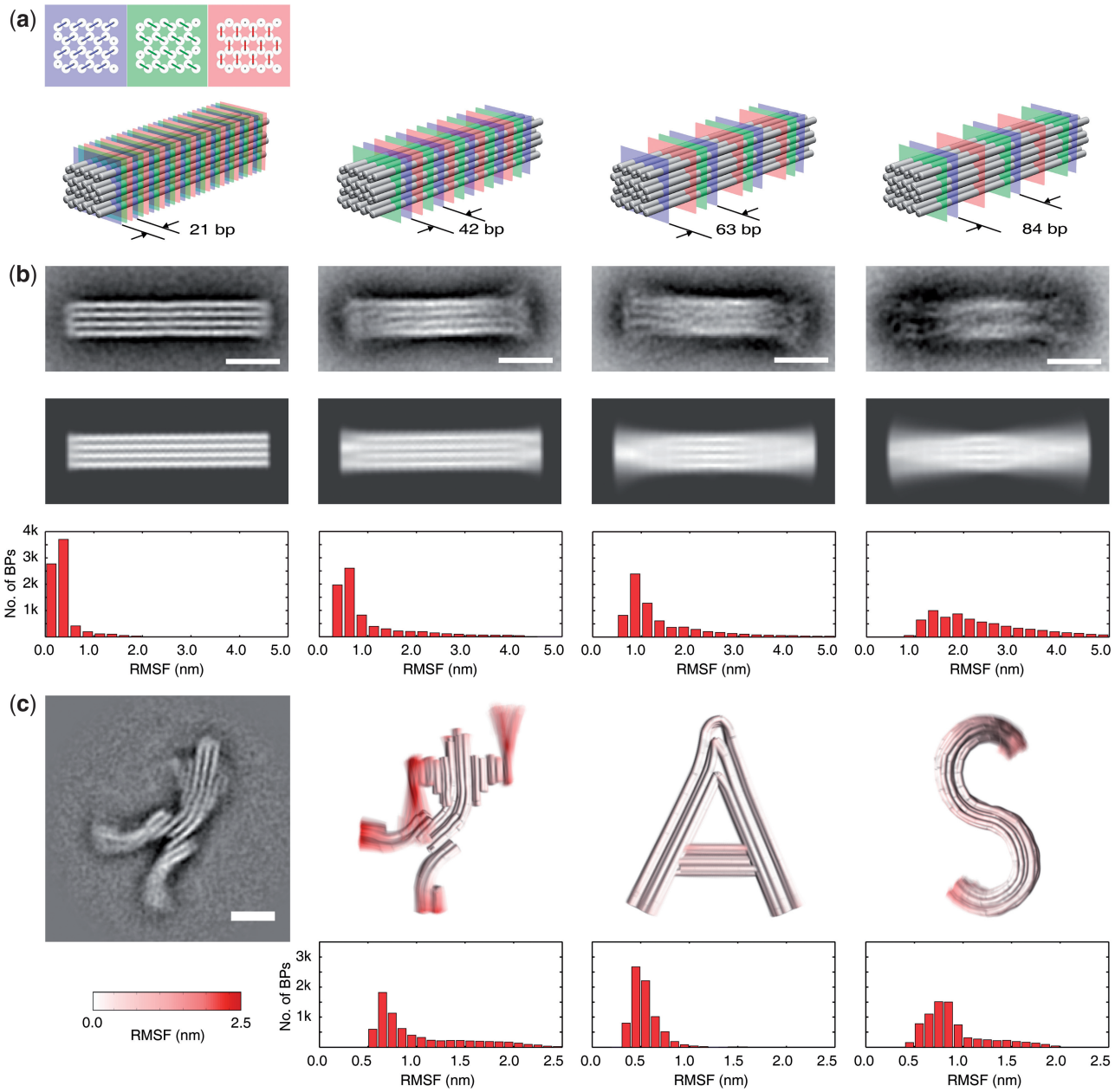

Figure 4. Experimental validation of the flexibility of DNA nanostructures. (**a**) 32-helix bundle objects packed on a honeycomb lattice with decreasing crossover density corresponding to axial spacings of 21 (1st column), 42 (2nd column), 63 (3rd column) and 84 (4th column) basepairs (Supplementary Figures S20–23). The inset depicts the three distinct crossover orientations in the honeycomb lattice. (**b**) Experimental (top) and simulated (middle) TEM images obtained from single-particle averaging (Supplementary Figures S10–S14), and (bottom) quantitative distributions in root-mean-square fluctuation amplitude. (**c**) 3D renderings and quantitative distributions in root-mean-square fluctuation amplitude of robot-like object (2nd column), letter 'A' (3rd column), and letter 'S' (4th column). TEM image of robot-like object (1st column) is obtained by averaging single particle images (Supplementary Figure S15).

lattice (21). In agreement with these published data, our model predicts a global twist deformation, with decreasing twist angle that results from the increasing torsional stiffness of blocks of increasing thickness (Supplementary Figure S6). Interestingly, for a single-layer rectangular design, the predicted shape exhibits overall bend in addition to twist due to the non-linear stretch-bend-twist energetic coupling that emerges at large twist angle (Figure 3d and Supplementary Figures S7–S8). Importantly, this coupling is not due to intrinsic mechanical coupling of these modes of deformation of the DNA double-helix itself, but rather the mechanical coupling of these degrees of freedom resulting from rigid crossovers that connect neighboring helices in the structure. 3D cryo-electron microscopy of free-standing structures will be required to validate this subtle model prediction. We validated the ability of our model to predict solution shapes more generally for a variety of complex shapes

including a previously published tensegrity motif (11), which, like the preceding wireframe structures, could not be analyzed using our previous modeling framework (1). Importantly, shape predictions are made correctly in a completely automatic, unsupervised manner without any feedback from the designer (Supplementary Figures S9 and S16), greatly enhancing the design–test–design cycle due to the elimination of the financially costly and time-consuming experimental validation step.

Thermal forces in solution tend to disorder nucleic acid nanostructures, potentially eliminating their ability to fulfill target function. The degree to which structural features match their target shape in solution, termed here 'mechanical integrity', is therefore a centrally important property to consider in nanostructure design. Notably, this feature of DNA origami structures is distinct from the question of folding stability of the structure, because it is concerned specifically with the question of what the flexibility or compliance of the folded, target structure is. One tunable structural parameter that is expected to influence mechanical integrity directly is the density of phosphate backbone crossovers that link double-helical DNA domains. To test the ability of our model to predict the effect of this design parameter on flexibility or integrity, we designed and built four versions of a 32-helix multi-layer DNA origami object in honeycomb-lattice packing with decreasing densities of crossovers linking neighboring double-helical domains (1 crossover per 21, 42, 63 and 84 bp) (Figure 4a). Negative-stain TEM micrographs illustrate the conformational variability of the resulting objects (Supplementary Figures S10–S14). Superposition of single-particle images illustrates the effect of decreasing crossover spacing on mean object conformation (Figure 4b), with objects becoming more polymorphic structurally as crossover density decreases.

We extended our framework to compute 'mean fluctuation micrographs' due to thermal fluctuations at 298 K to enable direct comparison with experiment. Again, visual correspondence within experimental error is achieved (Figure 4b). In contrast to experiment, however, the model enables direct quantitation of distributions of root-mean-square fluctuations (RMSFs) of individual basepairs within the bundle (Figure 4c). Obtaining such information experimentally is currently impossible. While agreement between model predictions and experiment are apparent, flexibility predictions are likely to represent a lower bound on true flexibility because they neglect unknown structural defects in DNA origami structures such as missing staple strands. Notwithstanding, the ability to predict flexibility of DNA-based nanostructures will be important to their design when specific local or global flexibilities are required, including in the design of monomers used to synthesize higher order polymers and tile-like structures (22,23).

Molecular self-assembly using DNA and other nucleic acids has great potential for building nanostructures for target applications in materials and biological science. A key challenge for leveraging this design modality in functional applications is the ability to design target shapes to meet desired geometrical and mechanical properties. The present computational approach that enables shape and mechanics prediction of DNA-based nanostructures assembled using principles of DNA origami demonstrates the capacity to predict not only solution shape but also structural flexibility, or mechanical integrity, at the nanoscale. We present here a new model for DNA origami that includes the ability to model wireframe structures, backbone nicks and single-stranded DNA used to design tensegrity structures. In addition to predicting complex 3D solution shape and flexibility that is validated experimentally for the first time here, our model reveals novel, subtle structural features of DNA origami objects including global out-of-plane deformations that require further experimental validation. These new modeling features are included in our online, web-based analysis tool CanDo (http://cando.dna-origami.org). We anticipate this predictive computational modeling framework will make important contributions to the future development of functional DNA nanostructures with applications in diverse areas of science and technology.

SUPPLEMENTARY DATA

Supplementary Data are available at NAR Online: Supplementary Note 1, Supplementary Figures S1–S23, and Supplementary References [24–25].

ACKNOWLEDGEMENTS

Discussions with Klaus-Jürgen Bathe (M.I.T.) and Arash Mahdavi (ADINA R&D, Inc.) are gratefully acknowledged. We thank Yonggang Ke and Tim Liedl for providing the caDNAno design files of 3D blocks on a square lattice and a tensegrity structure, respectively, and Shawn Douglas for help in interpreting the caDNAno design file format.

FUNDING

MIT Faculty Start-up Funds and the Samuel A. Goldblith Professorship (to M.B.); the Cluster for Integrated Protein Science Munich and a Hans-Fischer tenure track grant from TUM Institute for Advanced Study (to H.D.); a stipend from the TUM graduate school 'Materials at Complex Interfaces'(CompInt to F.K.); The Cluster for Integrated Protein Science Munich and Technische Universität München Institute for Advanced Study by the German Excellence Initiative; CompInt is funded by the state of Bavaria. Funding for open access charge: MIT Faculty Start-up Funds.

Conflict of interest statement. None declared.

REFERENCES

1. Castro,C.E., Kilchherr,F., Kim,D.-N., Shiao,E.L., Wauer,T., Wortmann,P., Bathe,M. and Dietz,H. (2011) A primer to scaffolded DNA origami. *Nat. Meth.*, **8**, 221–229.
2. Seeman,N.C. (2010) Nanomaterials Based on DNA. *Annu. Rev. Biochem.*, **79**, 65–87.
3. Jaeger,L. and Chworos,A. (2006) The architectonics of programmable RNA and DNA nanostructures. *Curr. Opin. Struct. Biol.*, **16**, 531–543.

4. Shih,W.M. and Lin,C. (2010) Knitting complex weaves with DNA origami. *Curr. Opin. Struct. Biol.*, **20**, 276–282.
5. Rothemund,P.W.K. (2006) Folding DNA to create nanoscale shapes and patterns. *Nature*, **440**, 297–302.
6. Douglas,S.M., Dietz,H., Liedl,T., Hogberg,B., Graf,F. and Shih,W.M. (2009) Self-assembly of DNA into nanoscale three-dimensional shapes. *Nature*, **459**, 414–418.
7. Dietz,H., Douglas,S.M. and Shih,W.M. (2009) Folding DNA into twisted and curved nanoscale shapes. *Science*, **325**, 725–730.
8. Andersen,E.S., Dong,M., Nielsen,M.M., Jahn,K., Subramani,R., Mamdouh,W., Golas,M.M., Sander,B., Stark,H., Oliveira,C.L.P. *et al.* (2009) Self-assembly of a nanoscale DNA box with a controllable lid. *Nature*, **459**, 73–76.
9. Han,D., Pal,S., Liu,Y. and Yan,H. (2010) Folding and cutting DNA into reconfigurable topological nanostructures. *Nat. Nano.*, **5**, 712–717.
10. Han,D., Pal,S., Nangreave,J., Deng,Z., Liu,Y. and Yan,H. (2011) DNA origami with complex curvatures in three-dimensional space. *Science*, **332**, 342–346.
11. Liedl,T., Hogberg,B., Tytell,J., Ingber,D.E. and Shih,W.M. (2010) Self-assembly of three-dimensional prestressed tensegrity structures from DNA. *Nat. Nano*, **5**, 520–524.
12. Tang,G., Peng,L., Baldwin,P.R., Mann,D.S., Jiang,W., Rees,I. and Ludtke,S.J. (2007) EMAN2: an extensible image processing suite for electron microscopy. *J. Struct. Biol.*, **157**, 38–46.
13. Hays,J.B. and Zimm,B.H. (1970) Flexibility and stiffness in nicked DNA. *J. Mol. Biol.*, **48**, 297–317.
14. Smith,S.B., Cui,Y. and Bustamante,C. (1996) Overstretching B-DNA: the elastic response of individual double-stranded and single-stranded DNA molecules. *Science*, **271**, 795–799.
15. Bathe,M. (2008) A finite element framework for computation of protein normal modes and mechanical response. *Proteins: Struct. Funct. Bioinform.*, **70**, 1595–1609.
16. Kim,D.-N., Nguyen,C.-T. and Bathe,M. (2011) Conformational dynamics of supramolecular protein assemblies. *J. Struct. Biol.*, **173**, 261–270.
17. McQuarrie,D.A. (1975) *Statistical Mechanics*. Harper & Row, New York.
18. Rief,M., Clausen-Schaumann,H. and Gaub,H.E. (1999) Sequence-dependent mechanics of single DNA molecules. *Nat. Struct. Mol. Biol.*, **6**, 346–349.
19. Douglas,S.M., Marblestone,A.H., Teerapittayanon,S., Vazquez,A., Church,G.M. and Shih,W.M. (2009) Rapid prototyping of 3D DNA-origami shapes with caDNAno. *Nucleic Acids Res.*, **37**, 5001–5006.
20. Bathe,K.J. (1996) *Finite Element Procedures*. Prentice Hall Inc., Upper Saddle River, New Jersey.
21. Ke,Y., Douglas,S.M., Liu,M., Sharma,J., Cheng,A., Leung,A., Liu,Y., Shih,W.M. and Yan,H. (2009) Multilayer DNA origami packed on a square lattice. *J. Am. Chem. Soc.*, **131**, 15903–15908.
22. Woo,S. and Rothemund,P.W.K. (2011) Programmable molecular recognition based on the geometry of DNA nanostructures. *Nat. Chem.*, **3**, 620–627.
23. Schulman,R. and Winfree,E. (2007) Synthesis of crystals with a programmable kinetic barrier to nucleation. *Proc. Natl. Acad. Sci. USA*, **104**, 15236–15241.
24. Bryant,Z., Stone,M.D., Gore,J., Smith,S.B., Cozzarelli,N.R. and Bustamante,C. (2003) Structural transitions and elasticity from torque measurements on DNA. *Nature*, **424**, 338–341.
25. Peters,J.P. and Maher,L.J. III (2010) DNA curvature and flexibility in vitro and in vivo. *Quart. Rev. Biophys.*, **43**, 23–63.